Pergamon

*Int. J. Solids Structures* Vol. 33, No. 29, pp. 4395–4409, 1996

Printed in Great Britain
0020-7683/96 $15.00 + .00

0020-7683(95)00231-6

# AN ANALYTICAL METHOD FOR FAILURE PREDICTION OF MULTI-FASTENER COMPOSITE JOINTS

Y. XIONG
Structures, Materials, and Propulsion Lab, Institute for Aerospace Research, National Research Council Canada, Ottawa, Canada K1A 0R6

(*Received* 12 *February* 1995; *in revised form* 15 *September* 1995)

**Abstract**—An analytical method is developed for failure prediction of composite bolted joints with multiple fasteners. The flexibility of all members in the joint is taken into account. A complex variational approach is proposed for the stress analysis of the component plates which involves multiple loaded holes and a strength of materials approach is used for the analysis of fasteners which are modeled as short elastic beams. These analyses are carried out in an iterative scheme which provides the stress distributions in the jointed plates. The failure strength and mode of the joint are predicted using the results from the joint analysis along with the well-known point stress criterion. The effectiveness of the analytical method developed is demonstrated by the comparisons made between the results of the present analysis for several joints and the data available in the literature. Crown Copyright © 1996 Published by Elsevier Science Ltd.

## 1. INTRODUCTION

The advanced fiber reinforced composite materials are increasingly used in the manufacturing of aerospace structures due to their high strength to weight ratios. In these structures, mechanically fastened joints are indispensable for the assembly of structural components. As a result, the development of efficient methods for the design and analysis of mechanically fastened composite joints has been the focus of numerous research over the years. Three major methods have been employed for composite joint strength analysis which included the finite element method, e.g., Chang *et al.* (1984) and Crews *et al.* (1981), the two dimensional anisotropic elastic analysis, e.g., De Jong (1977), and the boundary collocation method, e.g., Oplinger and Gandhi (1974) and more recently Madenci and Ileri (1993). Based on the boundary collocation method, Ramkumar *et al.* (1986, 1988) derived some special finite elements and used these elements for strength analysis of composite joints with multiple fasteners.

While the finite element method is a versatile numerical technique which can handle various geometry and hole patterns, it is not ideal for parametric studies or optimum design. The analytical method following Lekhnitskii (1968) uses an assumption of infinite plates and requires a finite width correction for an actual laminate of finite geometry. In addition, difficulties arise in laminates with arbitrarily located multiple loaded holes because of the interactions. The boundary collocation method usually involves a conformal mapping and a least-squares scheme. In the author's experience, the results from the boundary collocation method are sensitive to the selection of both the complex stress potentials and the boundary points and convergence to incorrect values is possible if the selection is inappropriate.

In the majority of the methods used for strength analysis of composite joints, the fasteners are assumed to be infinitely rigid. Force boundary conditions are usually used on the hole edges with an assumed distribution for the radial pressure. It has been recognized that the boundary conditions on the loaded hole and the fasteners' flexibility have great effects on the stress distribution around the hole. The use of a displacement boundary condition to represent the effect of the fastener bearing against the hole, Oplinger (1978), and the consideration of the fasteners' flexibility, Ramkumar *et al.* (1986), were found to give more accurate predictions.

In this paper, an analytical method is developed for the failure prediction of composite joints involving multiple fasteners. This method is being used in the development of a PC-based design model for composite joints involving multiple fasteners. In this method, the flexibility of all the joined members is taken into account by an iterative analysis scheme. A complex variational approach is proposed for the stress analysis of the joined plates. The approach is based on the complex equations of the problem and the variational principles. In this approach, the equilibrium equations and compatibility relation are satisfied exactly in the domain. All boundary conditions are satisfied through the variational formulations. While a displacement-based formulation is employed for one plate, a mixed formulation is used for the other plate. In the mixed formulation, displacement boundary conditions for the fastener holes are dealt with by introducing Lagrangian multipliers. In this way the actual load distributions on the holes transferred by the fasteners are determined, rather than assumed, from the Lagrangian multipliers in the formulation. The fasteners are modeled as elastic beams using a strength of materials approach. The joint failure strength and mode are predicted using the results of the joint stress analysis along with the point stress failure criterion, Whitney and Nuismer (1974). In this failure criterion, the concept of characteristic lines is introduced for the three failure modes: net-tension, bearing, and shear-out, respectively, which involves two independent characteristic dimensions. To verify the effectiveness of the analytical method developed, results of several testing cases and comparisons with the data available in the literature are presented.

## 2. STATEMENT OF PROBLEM

The problem under study is a composite-to-metal or composite-to-composite joint which involves two or three plates-joined by multiple fasteners. The configurations of single-lap (two plates) and double-lap joints (three plates) with two fasteners are illustrated in Figs 1 and 2, respectively. In the double-lap joint, Plate 1 and Plate 3 can be made of a metal or a composite. In the present problem, these two plates are assumed to be identical and hence only one plate is analyzed. Plate 2 is assumed to be made of a composite and its failure is to be predicted. The plates are of the same finite width, $W$. They have, in general, $m$ circular or elliptical loaded holes of various sizes which are arbitrarily located, as shown for Plate 2 in Fig. 3. The tensile load, $P$, applied at the edge of the middle plate, is in equilibrium with the $m$ fastener loads, $P_i$ $(i = 1, 2, \ldots, m)$. This load is transferred to Plate 1 in the single-lap joint. For the double-lap joint, this load is transferred to Plates 1 and 3. Since these two plates are identical, the load is evenly distributed between them.

It is noted that the actual stress state at the fastener location is complex and three dimensional in nature. This stress state is influenced by many factors concerning the

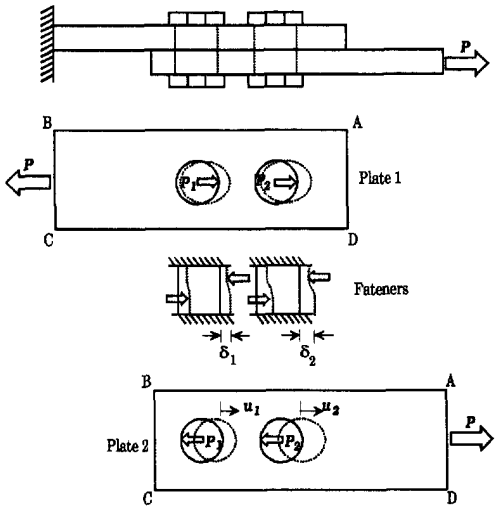


Fig. 1. Configuration of a single-lap joint.

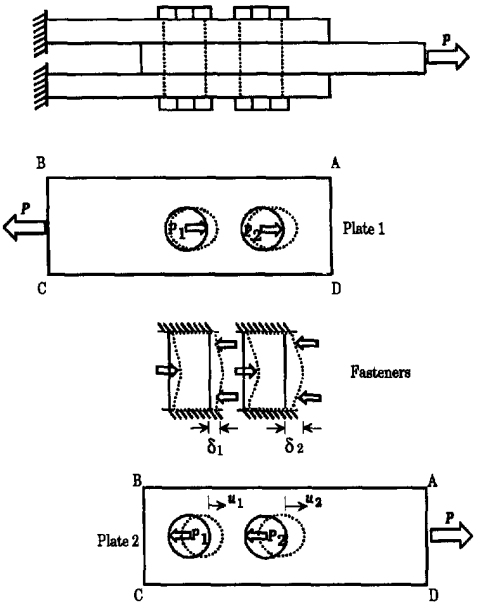


Fig. 2. Configuration of a double-lap joint.

properties of the fasteners and the bolted plates and their interactions. It would not be appropriate to take all these factors into account in developing a simple analytical facility for composite joints. The present paper considers symmetric configurations with respect to $x$-axis only and assumes: (i) the load on one plate is transferred by flexible frictionless fasteners over half of the hole edges along the primary loading direction, and (ii) the secondary bending of the plates due to load eccentricity is negligible compared to the in-plane deformations. Therefore in the present stress analysis for Plate 1 and Plate 2, general in-plane loading conditions are considered using two dimensional anisotropic elasticity. The fasteners are modeled as elastic beams with fixed end conditions for the double-lap joint. For the single-lap joint, the fasteners are fixed at one end and are allowed to translate

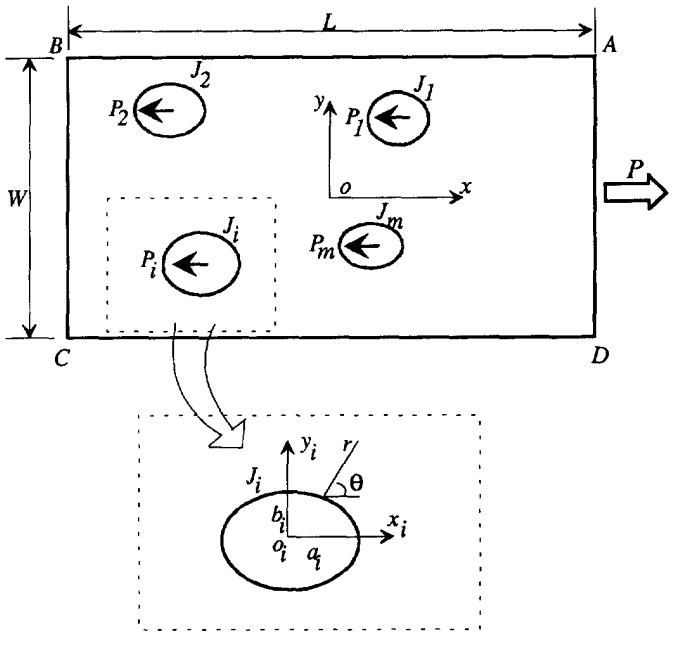


Fig. 3. General geometry configuration of Plate 2.

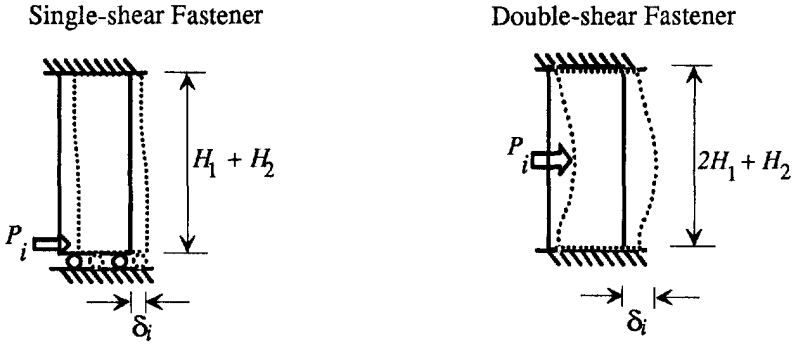


Fig. 4. Fasteners modeled as elastic beams.

in the loading direction at the other end, as shown in Fig. 4. In this way, the rotation of the fastener is simulated.

For the sake of simplicity, an identical set of notations is employed for both Plate 1 and Plate 2 as they are analyzed separately. The global coordinate system, $x$-$y$, is located at the center of the plate. The corresponding stress resultants and displacement components are denoted as $N_x$, $N_y$, $N_{xy}$, $u$, and $v$, respectively. The location of the $i$-th hole in the plate is specified by the coordinates of its origin $o_i$ $(x_{oi}, y_{oi})$. A local Cartesian system, $x_i$-$y_i$, is used for each hole which is coincident with the major and minor axes of the hole, $a_i$ and $b_i$. The local coordinate system for each hole is related to the global system as:

$$x_i = x - x_{oi}, \quad y_i = y - y_{oi}, \quad i = 1, 2, \ldots, m \tag{1}$$

In the local Cartesian system, the periphery of the $i$-th hole is expressed, in parametric form, as:

$$x_i = a_i \cos\beta, \quad y_i = b_i \sin\beta, \quad 0 \leqslant \beta \leqslant 2\pi \tag{2}$$

For the purpose of convenience, a polar system, $r$-$\theta$, is also used on the periphery of each fastener hole with the $r$-axis being the outer normal direction and $\theta = 0$ being the local $x_i$ axis. Noting the relation between the angle $\theta$ and the parameter $\beta$, the following transformations are established for the stress and displacement components

$$N_r = \frac{(N_x b_i^2 \cos^2\beta + N_y a_i^2 \sin^2\beta + 2N_{xy} a_i b_i \cos\beta \sin\beta)}{(a_i^2 \sin^2\beta + b_i^2 \cos^2\beta)}$$

$$N_\theta = \frac{(N_x a_i^2 \sin^2\beta + N_y b_i^2 \cos^2\beta - 2N_{xy} a_i b_i \cos\beta \sin\beta)}{(a_i^2 \sin^2\beta + b_i^2 \cos^2\beta)}$$

$$N_{r\theta} = \frac{[(-N_x + N_y) a_i b_i \cos\beta \sin\beta + N_{xy}(b_i^2 \cos^2\beta - a_i^2 \sin^2\beta)]}{(a_i^2 \sin^2\beta + b_i^2 \cos^2\beta)} \tag{3}$$

and

$$u_r = \frac{u b_i \cos\beta + v a_i \sin\beta}{\sqrt{a_i^2 \sin^2\beta + b_i^2 \cos^2\beta}}, \quad u_\theta = \frac{-u a_i \sin\beta + v b_i \cos\beta}{\sqrt{a_i^2 \sin^2\beta + b_i^2 \cos^2\beta}} \tag{4}$$

## 3. JOINT STRESS ANALYSIS

In order to determine the stress state in the joint, it is important to account for the interaction of all joined members. In this section, joint stress analysis is conducted which

takes into account the flexibility of the plates and fasteners. This is accomplished by an iterative scheme involving the relative deformation between the fasteners and plates.

### 3.1. *Iterative scheme*

As seen in Figures 1 and 2, the external load, $P$, applied on Plate 2 is transferred by the fasteners to Plate 1 (3). This load transfer results in the deflection of fasteners and the elongation of the holes in Plate 1 (3). The combined deformation due to fastener deflection and hole elongation affect, in turn, the deformation of Plate 2. This effect is dealt with by considering the rigid body motions of the fasteners. The contact region of each hole in Plate 2 is assumed to move a distance equal to the summation of the corresponding hole elongation in Plate 1 (3) and the deflection of the fastener. According to this mechanism, an iterative scheme which involves the following steps is established for joint stress analysis.

*Step* 1. Assign an initial value for each fastener load. Since the fastener load transferred is proportional to their bending stiffness, $EI$, the initial values assigned are:

$$P_i = \frac{E_i I_i}{E_1 I_1 + E_2 I_2 + \cdots + E_m I_m} P, \quad i = 1, 2, \ldots, m \tag{5}$$

which are in equilibrium with the externally applied load, $P$.

*Step* 2. Calculate the hole elongation in Plate 1 under the applied load and the fastener loads. The fastener loads are simulated by a cosine function. For a double-lap joint, Plate 1 is subjected to half of the applied load.

*Step* 3. Calculate the deflections of the fasteners under the shear loads transferred by the fasteners.

*Step* 4. Calculate the summation of hole elongations and fastener deflections in Plate 1. The combined deformation is taken as the rigid body movement of the contact region of the corresponding fastener holes in Plate 2. Calculate the reactions on holes of Plate 2 under the rigid body motions and the applied load, $P$.

*Step* 5. Take the reactions on the holes of Plate 2 as new fastener loads and repeat steps 2–4 until a convergent solution is obtained.

It is noted that in this scheme a displacement boundary condition is used in the analysis of Plate 2. As a result, the actual fastener loads are calculated rather than assumed. The following subsections describe, in detail, the equations used in each step.

### 3.2. *Basic complex equations for Plate* 1 *and Plate* 2

In the complex theory of the two dimensional anisotropic elasticity, all basic relations of the problem are described using the two stress potentials, $\varphi_1$ and $\varphi_2$, see Lekhnitskii (1968). They are expressed in terms of the two complex coordinate variables, $z_1$ and $z_2$, which are defined as:

$$z_1 = x + \mu_1 y, \quad z_2 = x + \mu_2 y \tag{6}$$

where $\mu_1$ and $\mu_2$ are the two distinct complex roots, with positive imaginary part, of the characteristic equation of the laminate. The equation is written, in terms of the in-plane compliance coefficients, $a_{ij}$ $(i,j = 1, 2, 6)$, as:

$$a_{11}\mu^4 - 2a_{16}\mu^3 + (2a_{12} + a_{66})\mu^2 - 2a_{26}\mu + a_{22} = 0 \tag{7}$$

In cases of a metallic plate where $\mu_1 = \mu_2 = \mu$, we can assume $\mu_1 = \mu - i\varepsilon$, and $\mu_2 = \mu + i\varepsilon$, where $\varepsilon \ll 1$. This assumption is considered acceptable for numerical computations.

The stress resultants take the following form:

$$N_x = 2\mathrm{Re}\left[\mu_1^2 \frac{\mathrm{d}\varphi_1(z_1)}{\mathrm{d}z_1} + \mu_2^2 \frac{\mathrm{d}\varphi_2(z_2)}{\mathrm{d}z_2}\right]$$

$$N_y = 2\mathrm{Re}\left[\frac{\mathrm{d}\varphi_1(z_1)}{\mathrm{d}z_1} + \frac{\mathrm{d}\varphi_2(z_2)}{\mathrm{d}z_2}\right]$$

$$N_{xy} = -2\mathrm{Re}\left[\mu_1 \frac{\mathrm{d}\varphi_1(z_1)}{\mathrm{d}z_1} + \mu_2 \frac{\mathrm{d}\varphi_2(z_2)}{\mathrm{d}z_2}\right] \tag{8}$$

and the corresponding displacement components are derived as:

$$u = 2\mathrm{Re}\left[p_1\varphi_1(z_1) + p_2\varphi_2(z_2)\right], \quad v = 2\mathrm{Re}\left[q_1\varphi_1(z_1) + q_2\varphi_2(z_2)\right] \tag{9}$$

where the two complex constants are defined as:

$$p_k = a_{11}\mu_k^2 + a_{12} - a_{16}\mu_k, \quad q_k = a_{12}\mu_k + a_{22}/\mu_k - a_{26}, \quad k = 1,2 \tag{10}$$

It is noted that the constants for the rigid body motions are set to zero in eqn (9) in order to avoid any rigid body motion for the whole plate. The stress resultants and displacement components are related by the constitutive equations as:

$$N_x = A_{11}\frac{\partial u}{\partial x} + A_{12}\frac{\partial v}{\partial y} + A_{16}\left(\frac{\partial u}{\partial y} + \frac{\partial v}{\partial x}\right)$$

$$N_y = A_{12}\frac{\partial u}{\partial x} + A_{22}\frac{\partial v}{\partial y} + A_{26}\left(\frac{\partial u}{\partial y} + \frac{\partial v}{\partial x}\right)$$

$$N_{xy} = A_{16}\frac{\partial u}{\partial x} + A_{26}\frac{\partial v}{\partial y} + A_{66}\left(\frac{\partial u}{\partial y} + \frac{\partial v}{\partial x}\right) \tag{11}$$

where $A_{ij}$ $(i,j = 1,2,6)$ are the in-plane stiffness coefficients, that is $[A_{ij}]^{-1}$ is equal to $[a_{ij}]$.

It is known that the stress and displacement components expressed in terms of the two stress potentials as in eqns (8) and (9) satisfy the equilibrium equations and the compatibility relation in the domain of the plate. The problem is now to find the appropriate stress potentials so that the respective boundary conditions are satisfied. For this purpose, a displacement-based formulation and a mixed variational formulation are established using the above complex equations for Plate 1 and Plate 2, respectively. Then the admissible functions in these formulations are the two complex stress potentials which are selected in a summation of truncated Laurent series with conformal mapping as:

$$\varphi_1 = C_{10} + \sum_{n=1}^{N} C_{1n} z_1^n + \sum_{i=1}^{m}\left(D_{10}^i \ln \zeta_{1i} + \sum_{n=1}^{N} D_{1n}^i \zeta_{1i}^{-n}\right)$$

$$\varphi_2 = C_{20} + \sum_{n=1}^{N} C_{2n} z_2^n + \sum_{i=1}^{m}\left(D_{20}^i \ln \zeta_{2i} + \sum_{n=1}^{N} D_{2n}^i \zeta_{2i}^{-n}\right) \tag{12}$$

where the undetermined constants $C_{1n}$, $D_{1n}^i$, $C_{2n}$, $D_{2n}^i$ are, in general, complex and the mapping functions, with transformations of coordinates, are:

$$\zeta_{ki} = \frac{[(x-x_{oi}) + \mu_k(y-y_{oi})] \pm \sqrt{[(x-x_{oi}) + \mu_k(y-y_{oi})]^2 - a_i^2 - b_i^2\mu_k^2}}{a_i - b_i\mu_k\sqrt{-1}}$$

$$k = 1,2, \quad i = 1,2,\ldots,m \tag{13}$$

where the sign of the square root term is chosen such that the $i$-th elliptical hole is mapped to a unit circle. Noting that the stress potentials in eqn (12) involve logarithm terms, the following conditions are imposed to ensure single-valued displacement components:

$$\mathrm{Im}\,(p_1 D^i_{10} + p_2 D^i_{20}) = 0, \quad \mathrm{Im}\,(q_1 D^i_{10} + q_2 D^i_{20}) = 0, \quad i = 1, 2, \ldots, m \tag{14}$$

The above outlined complex equations are considered valid for both Plate 1 and Plate 2. In the following analysis, the same set of notation is used for the two plates. To avoid confusion, the notation used in Section 3.3 refers to the variables of Plate 1 and the notation used in Section 3.5 refers to those of Plate 2.

3.3. *Displacement-based variational formulation for Plate* 1

As seen in Figs 1 and 2, Plate 1 is under the applied load, $P$, and the fastener loads, $P_i$. This problem involves only force boundary conditions which are written, for the $i$-th hole, as:

$$\begin{aligned} &N^i_r(\beta) = -p^i_r(\beta), \quad N^i_{r\theta}(\beta) = 0, && -\frac{\pi}{2} \leqslant \beta \leqslant \frac{\pi}{2} \\ &N^i_r(\beta) = N^i_{r\theta}(\beta) = 0, && \frac{\pi}{2} \leqslant \beta \leqslant \frac{3\pi}{2} \end{aligned} \tag{15}$$

where $p^i_r(\beta)$ represents the radial pressure resulting from the fastener loading which is assumed to be a cosine distribution shown in the following equation:

$$p^i_r(\beta) = \frac{2P_i}{\pi b_i}\cos\beta \tag{16}$$

For completeness, the boundary conditions on the exterior edges are written as:

$$\begin{aligned} &\text{On edges A–B and C–D:} && N_y\left(x, \pm\frac{W}{2}\right) = N_{xy}\left(x, \pm\frac{W}{2}\right) = 0 \\ &\text{On edge B–C:} && N_x\left(-\frac{L}{2}, y\right) = \frac{P}{W}, \quad N_{xy}\left(-\frac{L}{2}, y\right) = 0 \\ &\text{On edge D–A:} && N_x\left(\frac{L}{2}, y\right) = N_{xy}\left(\frac{L}{2}, y\right) = 0 \end{aligned} \tag{17}$$

Since Plate 1 does not have any displacement boundary conditions, the minimum potential energy theorem is applied. The total potential energy of Plate 1 is written as:

$$\begin{aligned} \tilde{\Pi}_1 = \frac{1}{2}\int_\Omega \Bigg\{ & A_{11}\left(\frac{\partial u}{\partial x}\right)^2 + 2A_{12}\frac{\partial u}{\partial x}\frac{\partial v}{\partial y} + A_{22}\left(\frac{\partial v}{\partial y}\right)^2 \\ & + 2\left(A_{16}\frac{\partial u}{\partial x} + A_{26}\frac{\partial u}{\partial x}\right)\left(\frac{\partial u}{\partial y} + \frac{\partial v}{\partial x}\right) + A_{66}\left(\frac{\partial u}{\partial y} + \frac{\partial v}{\partial x}\right)^2 \Bigg\} \mathrm{d}x\,\mathrm{d}y \\ & - \int_{y_B}^{y_C} \frac{P}{W} u|_{x=-L/2}\,\mathrm{d}y - \sum_{i=1}^{m} \int_{\pi/2}^{\pi/2} p^i_r(\beta) u_r(\beta) \sqrt{a_i^2 \sin^2\beta + b_i^2 \cos^2\beta}\,\mathrm{d}\beta \end{aligned} \tag{18}$$

where $\Omega$ denotes the domain of Plate 1. Using the integration by parts, the first order variation of the above energy functional with respect to $u$ and $v$, respectively, is derived and written as:

$$\delta\tilde{\Pi}_1 = \int_\Omega \left[ -\left(\frac{\partial N_x}{\partial x} + \frac{\partial N_{xy}}{\partial y}\right)\delta u - \left(\frac{\partial N_{xy}}{\partial x} + \frac{\partial N_y}{\partial y}\right)\delta v \right] \mathrm{d}x\,\mathrm{d}y + \text{boundary terms} \tag{19}$$

where the constitutive relations shown in eqn (11) are used to simplify the expressions of the stress resultants. Note that all the stress and displacement components are actually related to the two stress potentials, $\varphi_1$ and $\varphi_2$.

The above variational formulation involves one area integration along with boundary terms. Associated with the area integration are the two equilibrium equations which are satisfied automatically by using the stress potentials. Therefore the area integration in eqn (19) vanishes. Then the variational formulation involves only boundary terms which are written, in an expanded form, as:

$$\begin{aligned}
\delta\tilde{\Pi}_1 = & -\int_{x_A}^{x_B} (N_{xy}\delta u + N_y \delta v)|_{y=W/2}\,\mathrm{d}x + \int_{y_B}^{y_C} \left[\left(N_x - \frac{P}{W}\right)\delta u + N_{xy}\delta v\right]\Big|_{x=-L/2} \mathrm{d}y \\
& - \int_{x_C}^{x_D} (N_{xy}\delta u + N_y \delta v)|_{y=-W/2}\,\mathrm{d}x + \int_{y_D}^{y_A} (N_x \delta u + N_{xy}\delta v)|_{x=L/2}\,\mathrm{d}y \\
& - \sum_{i=1}^{m} \left\{ \int_{-\pi/2}^{\pi/2} [(N_r^i - p_r^i)\delta u_r^i + N_{r\theta}^i \delta u_\theta^i] \sqrt{a_i^2 \sin^2\beta + b_i^2 \cos^2\beta}\,\mathrm{d}\beta \right. \\
& \left. + \int_{\pi/2}^{3\pi/2} (N_r^i \delta u_r^i + N_{r\theta}^i \delta u_\theta^i) \sqrt{a_i^2 \sin^2\beta + b_i^2 \cos^2\beta}\,\mathrm{d}\beta \right\}
\end{aligned} \tag{20}$$

It is seen that associated with the boundary integrations in eqn (20) are expressions for the boundary conditions along the interior and exterior edges, as in eqns (15) and (17). As a result, the minimization of the total potential energy is equivalent to the satisfaction of the required boundary conditions. This equation is written as:

$$\delta\tilde{\Pi}_1 = 0 \tag{21}$$

Using the stress potentials in eqn (12) as the trial functions for eqn (21), the complex constants are determined and then the stress distribution and deformation in Plate 1 are calculated. The hole elongations in this plate are to be used in the analysis of Plate 2, which can be calculated, from eqn (9), as:

$$u_i = 2\mathrm{Re}\,[p_1\varphi_1(x_{oi} + a_i + \mu_1 y_{oi}) + p_2\varphi_2(x_{oi} + a_i + \mu_2 y_{oi})] \quad i = 1, 2, \ldots, m \tag{22}$$

### 3.4. *Deflection of fasteners*

The fasteners are modeled as elastic beams and analyzed using the strength of materials approach, Timoshenko and Gere (1972). Failure is assumed not to occur in the fasteners. Since the fasteners are short, shear effects are taken into account. Although the fasteners are actually elastically supported, the boundary conditions of the fasteners are simplified, as shown in Fig. 4. The effect of elastic end supports is considered using a coefficient, $\eta_i$. As mentioned earlier, the load eccentricity in a single-lap joint is ignored in this work.

A fastener in a single-lap joint has a fixed end and a free end where the shear load is applied. The largest deflection in this case is:

$$\delta_i = \eta_i \frac{P_i(H_1 + H_2)^3}{12E_iI_i}\left[1 + \frac{12\alpha_s E_i I_i}{G_i A_i (H_1 + H_2)^2}\right], \quad i = 1, 2, \ldots, m \tag{23}$$

where $\alpha_s$ is the shear coefficient which is 1.33 for a circular cross section, $H$ denotes the thickness of the plate, $E_iI_i$ and $G_iA_i$ are the bending and shear rigidity, respectively, and $\eta_i$

is the coefficient accounting for effects of elastic end supports. For circular fasteners, the value of $\eta_i$ is taken as:

$$\eta_i = \left(\frac{d_i}{H_1}\right)^2, \quad i = 1, 2, \ldots, m \tag{24}$$

where $d_i$ is the diameter of the circular cross section and $H_1$ is the thickness of Plate 1. Equation (24) indicates that the deflection of a fastener decreases as Plate 1 becomes thicker.

In a double-lap joint, the fastener has both ends fixed and is subjected to a shear load at the mid-span, see Fig. 4. The largest deflection is:

$$\delta_i = \eta_i \frac{P_i(2H_1 + H_2)^3}{192E_iI_i}\left[1 + \frac{48\alpha_s E_i I_i}{G_i A_i (2H_1 + H_2)^2}\right], \quad i = 1, 2, \ldots, m \tag{25}$$

The fastener deflections calculated in eqns (23) and (25) produce a relative movement of the bolted plates which is taken into account in the analysis of Plate 2.

3.5. *Mixed variational formulation for Plate 2*

As seen in Figs 1 and 2, Plate 2 is under the applied load, $P$, and the fastener loads, $P_i$. In addition, each fastener hole in this plate has a rigid body motion which is equal to the summation of the hole elongation in Plate 1 and the fastener deflection:

$$\bar{u}_i = u_i + \delta_i, \quad i = 1, 2, \ldots, m \tag{26}$$

where $u_i$ is from eqn (22) and $\delta_i$ is from eqn (23) or (25). Since only the relative displacement is of interest, the rigid body motion of each hole is defined as the difference between the movement of the current hole and that of a reference hole. For convenience of analysis, this relative displacement in global $x$ direction is transferred into that in the outer normal direction on the hole edge, from eqn (4), as:

$$\bar{u}_r^i(\beta) = \frac{\bar{u}_i b_i \cos\beta}{\sqrt{a_i^2 \sin^2\beta + b_i^2 \cos^2\beta}}, \quad i = 1, 2, \ldots, m \tag{27}$$

Plate 2 involves both displacement and force boundary conditions which are written, for the $i$-th representative hole, as:

$$\begin{aligned} &N_r^i(\beta) = N_{r\theta}^i(\beta) = 0, && -\frac{\pi}{2} \leqslant \beta \leqslant \frac{\pi}{2} \\ &u_r^i(\beta) = \bar{u}_r^i(\beta), \quad N_{r\theta}^i(\beta) = 0, && \frac{\pi}{2} \leqslant \beta \leqslant \frac{3\pi}{2} \end{aligned} \tag{28}$$

and for exterior edges, as:

$$\begin{aligned} &\text{On edges A–B and C–D:} && N_y\left(x, \pm\frac{W}{2}\right) = N_{xy}\left(x, \pm\frac{W}{2}\right) = 0 \\ &\text{On edge B–C:} && N_x\left(-\frac{L}{2}, y\right) = N_{xy}\left(-\frac{L}{2}, y\right) = 0 \\ &\text{On edge D–A:} && N_x\left(\frac{L}{2}, y\right) = \frac{P}{W}, \quad N_{xy}\left(\frac{L}{2}, y\right) = 0 \end{aligned} \tag{29}$$

In the present case, a mixed variational formulation is applied. The functional in the formulation is derived from that of the minimum potential energy theorem with the displacement boundary conditions released by introducing Lagrangian multipliers, $\lambda^i$. The mixed functional is written as:

$$\begin{aligned}\tilde{\Pi}_2 = &\frac{1}{2}\int_\Omega \left\{A_{11}\left(\frac{\partial u}{\partial x}\right)^2 + 2A_{12}\frac{\partial u}{\partial x}\frac{\partial v}{\partial y} + A_{22}\left(\frac{\partial v}{\partial y}\right)^2\right.\\ &\left. + 2\left(A_{16}\frac{\partial u}{\partial x} + A_{26}\frac{\partial u}{\partial x}\right)\left(\frac{\partial u}{\partial y} + \frac{\partial v}{\partial x}\right) + A_{66}\left(\frac{\partial u}{\partial y} + \frac{\partial v}{\partial x}\right)^2\right\} \mathrm{d}x\,\mathrm{d}y\\ &- \int_{y_D}^{y_A} \frac{P}{W} u|_{x=L/2}\,\mathrm{d}y + \sum_{i=1}^{m}\int_{\pi/2}^{3\pi/2} \lambda^i(\beta)[u_r(\beta) - \bar{u}_r^i]\sqrt{a_i^2\sin^2\beta + b_i^2\cos^2\beta}\,\mathrm{d}\beta \end{aligned} \tag{30}$$

where $\Omega$ denotes the domain of Plate 2, $\lambda^i(\beta)$ is the Lagrangian Multiplier for the $i$-th hole. Using similar procedures in Section 3.3, the first order variation of the above energy functional with respect to $u$, $v$, and $\lambda^i$, respectively, is derived and written as:

$$\begin{aligned}\delta\tilde{\Pi}_2 = &-\int_{x_A}^{x_B} (N_{xy}\delta u + N_y\delta v)|_{y=W/2}\,\mathrm{d}x + \int_{y_B}^{y_C} (N_x\delta u + N_{xy}\delta v)|_{x=-L/2}\,\mathrm{d}y\\ &-\int_{x_C}^{x_D} (N_{xy}\delta u + N_y\delta v)|_{y=-W/2}\,\mathrm{d}x + \int_{y_D}^{y_A}\left[\left(N_x - \frac{P}{W}\right)\delta u + N_{xy}\delta v\right]\Big|_{x=L/2}\mathrm{d}y\\ &-\sum_{i=1}^{m}\left\{\int_{-\pi/2}^{\pi/2} (N_r^i\delta u_r^i + N_{r\theta}^i\delta u_\theta^i)\sqrt{a_i^2\sin^2\beta + b_i^2\cos^2\beta}\,\mathrm{d}\beta\right.\\ &\left.+\int_{\pi/2}^{3\pi/2}[(N_r^i - \lambda^i)\delta u_r^i - (u_r^i - \bar{u}_r^i)\delta\lambda^i + N_{r\theta}^i\delta u_\theta^i]\sqrt{a_i^2\sin^2\beta + b_i^2\cos^2\beta}\,\mathrm{d}\beta\right\}\end{aligned} \tag{31}$$

It is seen that associated with the boundary integrations in eqn (31) are expressions for the boundary conditions along the interior and exterior edges, as in eqns (28) and (29). The term associated with $\delta u_r^i$ reveals that the Lagrangian multiplier for each hole represents the corresponding radial stress on the loaded half of the hole edge. As a result, the vanishing condition of eqn (31) is equivalent to the satisfaction of all the boundary conditions of the present problem. This vanishing condition is written as:

$$\delta\tilde{\Pi}_2 = 0 \tag{32}$$

The solution of the problem is now to select appropriate stress potentials, $\varphi_1$ and $\varphi_2$, and Lagrangian Multipliers, $\lambda^i$, as the trial functions. While eqn (12) is used for the stress potentials, a general series form of trigonometric functions with undetermined real constants is selected for the Lagrangian Multipliers. This series is written as:

$$\lambda^i(\beta) = \lambda_1^i + \sum_{j=1}^{J}[\lambda_{2j}^i\sin(j\beta) + \lambda_{2j+1}^i\cos(j\beta)], \quad i = 1,2,\ldots,m \tag{33}$$

where the number of terms in this series is taken as $J = N-1$ in order for the series to be compatible with the stress functions expressed in eqn (12). Since the Lagrangian multipliers represent the radial pressure on the loaded half of the holes, the conditions of equilibrium in the global $x$ and $y$ directions are imposed in order to ensure the convergence of the computation. These conditions are written as:

$$\sum_{i=1}^{m}\int_{\pi/2}^{3\pi/2}\lambda^{i}(\beta)b_i\cos\beta\,\mathrm{d}\beta = P,\quad \sum_{i=1}^{m}\int_{\pi/2}^{2\pi/2}\lambda^{i}(\beta)a_i\sin\beta\,\mathrm{d}\beta = 0 \tag{34}$$

There are $2(m+1)(N+1)$ complex constants in eqn (12) and $m(J+1)$ real constants in eqn (33) which must be determined. This determination is accomplished by using eqn (32) along with conditions in eqns (14) and (34). Once these constants are determined, the stress and displacement components are calculated.

The fastener load on the $i$-th hole is determined by the integration:

$$P_i = \int_{\pi/2}^{3\pi/2}\lambda^{i}(\beta)b_i\cos\beta\,\mathrm{d}\beta,\quad i = 1,2,\ldots,m \tag{35}$$

The fastener loads calculated from eqn (35) are substituted back in the analyses for Plate 1 and the fasteners. This iteration proceeds until a convergent solution is obtained. The stress distributions in the vicinity of loaded holes in both Plate 1 and Plate 2 are then calculated and used for joint failure prediction.

## 4. JOINT FAILURE PREDICTION

With results of joint stress analysis at hand, the joint failure strength and mode can now be predicted. For the sake of simplicity, only the failure prediction of Plate 2 is outlined in this paper. Failure modes in composite joints can be very complex and quite different from those in metal joints because composites exhibit anisotropic properties, lack of ductility, and inherent interlaminar weakness. Three typical failure modes are considered in this work which are net-tension, bearing and shear-out. The point stress failure criterion developed by Whitney and Nuismer (1974) is employed which states that failure occurs when the maximum tensile stress, the maximum compressive stress, or the maximum shear stress at discrete locations on any of the loaded holes reaches the corresponding failure strength of the unnotched laminate. Two independent characteristic dimensions, $d_o^t$ and $d_o^b$, are required to specify the locations where the stress components are assessed, as shown in Fig. 5. The characteristic dimensions are usually determined from testing data. The point stress failure criterion can be expressed, for the $i$-th hole, as:

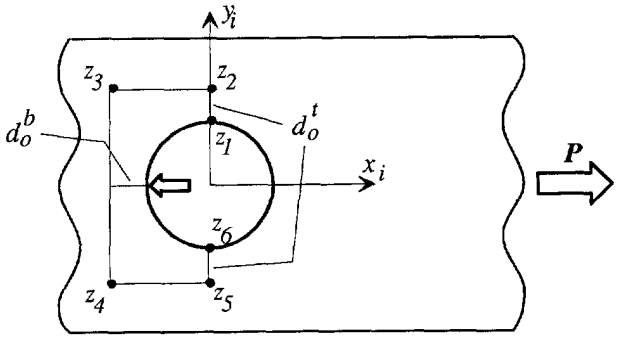


Net-tension line: $z_1$ - $z_2$ and $z_5$ - $z_6$

Shear-out line: $z_2$ - $z_3$ and $z_4$ - $z_5$

Bearing line: $z_3$ - $z_4$

Fig. 5. Characteristic dimensions in failure criterion.

$$\begin{aligned}
&\text{net-tension:} && \text{when } N_x(x,y)/H_2 = \bar{X} && \text{at} && x = x_{oi}, && y = y_{oi} \pm (b_i + d_o^t)\\
&\text{shear-out:} && \text{when } N_{xy}(x,y)/H_2 = \bar{S} && \text{at} && x = x_{oi} - (a_i + d_o^b), && y = y_{oi} \pm (b_i + d_o^t)\\
&\text{bearing:} && \text{when } N_x(x,y)/H_2 = \bar{X}' && \text{at} && x = x_{oi} - (a_i + d_o^b), && y = y_{oi}
\end{aligned} \tag{36}$$

where $\bar{X}$, $\bar{X}'$, and $\bar{S}$ are the failure strength of the corresponding unnotched laminate under uniaxial tension, uniaxial compression, and pure shear, respectively. These unnotched failure strengths can be determined empirically or calculated using the concepts of progressive ply failure and material degradation.

Since the stress components in the bolted plate are calculated from eqn (8) under the applied load, $P$, the joint strength for each failure mode can be determined using the following expressions:

$$\begin{aligned}
&\text{net-tension:} && \sigma_f^t = \frac{P/W}{N_x[x_{oi}, y_{oi} \pm (b_i + d_o^t)]}\bar{X}\\
&\text{shear-out:} && \sigma_f^s = \frac{P/W}{N_{xy}[x_{oi} - (a_i + d_o^b), y_{oi} \pm (b_i + d_o^t)]}\bar{S}\\
&\text{bearing:} && \sigma_f^b = \frac{P/W}{N_x[x_{oi} - (a_i + d_o^b), y_{oi}]}\bar{X}'
\end{aligned} \tag{37}$$

The prevailing joint strength and failure mode are identified from the minimum value of the three joint strengths calculated.

## 5. RESULTS AND DISCUSSION

Strength analysis of a set of composite-to-metal joints with multiple fasteners has been conducted using the analytical method developed and part of these results are presented in this section to demonstrate the effectiveness of the method. The joints analysed have been investigated theoretically and experimentally by Ramkumar *et al.* (1986, 1988). In all cases under study, Plate 1(3) is made of aluminum and Plate 2 is made of the material AS1/3501-6 with various lay-ups. All fasteners are steel with protruding heads. The material properties for each ply of AS1/3501-6 are: $E_L = 18.5 \times 10^6$ psi, $E_T = 1.9 \times 10^6$ psi, $G_{LT} = 0.85 \times 10^6$ psi, $\nu_{LT} = 0.3$, and the strength allowances are: $X = 230.0 \times 10^3$ psi, $X' = 321.0 \times 10^3$ psi, $Y = 9.5 \times 10^3$ psi, $Y' = 38.9 \times 10^3$ psi, $S = 17.3 \times 10^3$ psi. The material properties for aluminum and steel are taken as $E_{al} = 10 \times 10^6$ psi, $\nu_{al} = 0.3$ and $E_{st} = 30 \times 10^6$ psi, $\nu_{st} = 0.3$, respectively.

In the first case, the stresses in a four-fastener joint, as shown in Fig. 6, are calculated using the present method and by a finite element method involving gap elements. The

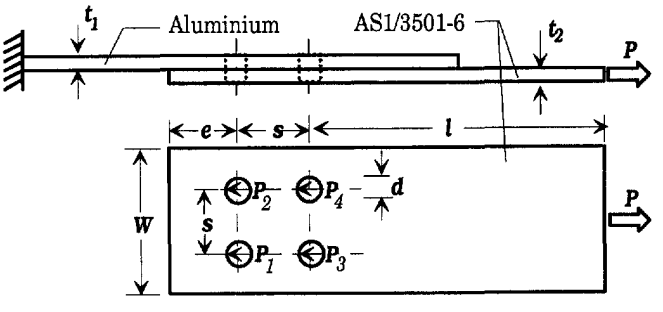


Fig. 6. Configuration of four-fastener joint.

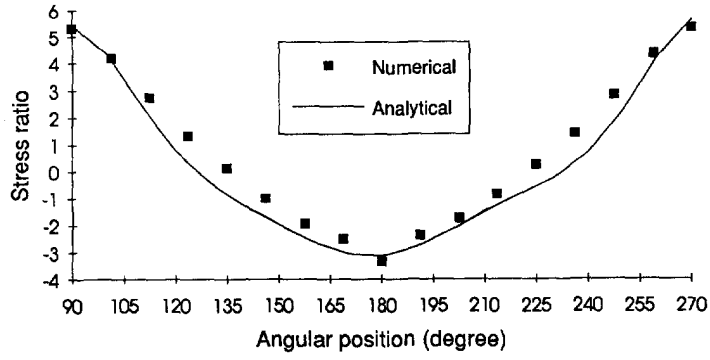


(i) Hoop stress around hole 3.

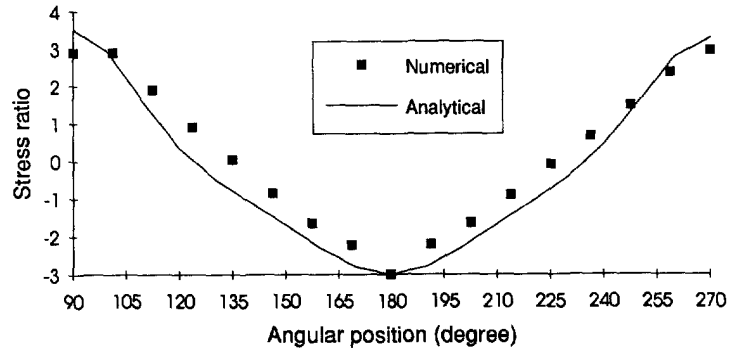


(ii) Hoop stress around hole 1.

Fig. 7. Comparison of stress results between analytical and FE methods.

layup of the composite laminate is $[(45/0/-45/0)_2/0/90]_s$. The distributions of the stress component in the loading direction around two fastener holes are shown in Fig. 7. The reasonably good agreement between the present results and the finite element data demonstrates the accuracy of the complex variational approach proposed for the joint stress analysis. Note that the discrepancies in the comparisons are due to the relatively coarse mesh used in the finite element model. Another reason for the discrepancies might be related to the ignorance of the pin displacements in the $y$-direction.

The failure strength and mode of the same joint are predicted using the values for the characteristic dimensions as: $d_o^t = 0.032$ in, $d_o^b = 0.032$ in. The fastener loads, joint failure load, failure location, and failure mode predicted from the present method are compared with the testing data and the SAMCJ predictions from Ramkumar *et al.* (1986, 1988). Good agreement is shown in Table 1 for this comparison. It is noted that the present method predicts the two lower failure modes as shear-out and net-tension. Since the failure strengths for these two modes are very close, the joint is predicted to fail in a combination of shear-out and net-tension as observed in the test.

As a final example, a double-lap joint with five fasteners in series is analyzed with the characteristic dimensions as: $d_o^t = 0.020$ in, $d_o^b = 0.020$ in. The joint configuration is shown in Fig. 8 and the layup of the composite laminate is $[(45/0/-45/0)_2/0/90]_{2s}$. Good agreement in the comparison of results is obtained, as shown in Table 2. The joint is predicted to fail in a single mode, net-tension, as the failure strengths of the other two modes are much higher than that for the net-tension mode. This prediction is identical to the test result.

Table 1. Fastener loads, failure load, location and mode of the four-fastener joint

| | Present prediction | SMACJ Ramkumar (1988) | Testing Ramkumar (1988) |
|---|---|---|---|
| $P_1/P$ | 0.23 | 0.24 | 0.25 |
| $P_2/P$ | 0.23 | 0.24 | 0.25 |
| $P_3/P$ | 0.27 | 0.26 | 0.29 |
| $P_4/P$ | 0.27 | 0.26 | 0.21 |
| $P_f$ ($\times 10^3$ lb) | 17.0 (17.7)* | 18.1 (18.9)* | 17.1 |
| Location | 3, 4 | 4 (3) | 3, 4 |
| Mode | shear-out (net tension) | shear-out | shear-out net-tension delamination |

* Possible failure mode at a slightly higher load level.

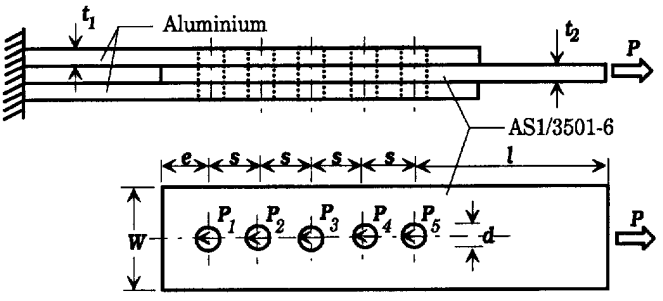


Fig. 8. Configuration of five-fastener joint.

Table 2. Fastener loads, failure load, location and mode of five-fastener joint

| | Present prediction | SAMCJ Ramkumar (1988) | Testing Ramkumar (1988) |
|---|---|---|---|
| $P_1/P$ | 0.164 | 0.172 | 0.164 |
| $P_2/P$ | 0.120 | 0.156 | 0.124 |
| $P_3/P$ | 0.133 | 0.167 | 0.161 |
| $P_4/P$ | 0.205 | 0.211 | 0.207 |
| $P_5/P$ | 0.379 | 0.293 | 0.345 |
| $P_f$ ($\times 10^3$lb) | 16.9 | 13.4 | 17.7 |
| Location | 5 | 5 | 5 |
| Mode | net-tension | net-tension | net-tension |

## 6. CONCLUSIONS

An analytical method has been developed for the failure prediction of composite joints involving multiple fasteners. An iterative scheme based on a complex variational approach was established. The proposed complex variational approach dealt with finite jointed plates involving multiple loaded holes with no requirement for finite width correction. The loaded holes were, in general, of elliptical shape and arbitrarily located in the plate and the fastener loads were determined, rather than assumed, from the Lagrangian multipliers introduced into the formulation. While the friction on the fastener-hole surfaces was ignored, the flexibility of the fasteners was taken into account by modeling the fasteners as elastic beams. The approach provided closed-form expressions for the stress resultants and displacement components and its accuracy was assessed by comparing the present calculation with the finite element results. In the prediction of joint failure strength and mode, the well-known point stress criterion was employed. The successful comparisons between the present predictions and the data available in the literature verified the effectiveness of the analytical method developed. More results of joint design using this method have been obtained and presented in Xiong and Poon (1994).

*Acknowledgements*—This work was carried out under IAR Program 3G3, Aerospace Structures, Structural Dynamics and Acoustics, Project/Sub-Project JGM-02 Mechanical Joining of Composite Structures.

## REFERENCES

Chang, Fu-Kuo, Scott, R. A. and Springer, G. S. (1984). Strength of bolted joints in laminated composites. AFWAL-TR-84-4029.

Crews, Jr., J. H., Hong, C. S. and Raju, I. S. (1981). Stress-concentration factors for finite orthotropic laminates with a pin-loaded hole. NASA Technical Paper 1862.

De Jong, Th. (1977). Stresses around pin-loaded holes in elastically orthotropic or isotropic plates. *J. Comp. Mat.* **11,** 313–331.

Lekhnitskii, S. G. (1968). *Anisotropic Plates*, Gordon and Breach Science Publishers, New York.

Madenci, E. and Ileri, L. (1993). Analytical determination of contact stresses in mechanically fastened composite laminates with finite boundaries. *Int. J. Solids Structures* **30,** 2469–2484.

Oplinger, D. W. and Gandhi, K. R. (1974). Stresses in mechanically fastened orthotropic laminates. AFFDL-TR-74-103, 811–842.

Oplinger, D. W. (1978). On the structural behaviour of mechanically fastened joints in composite structures. In *Proc. Conf. Fibrous Composites in Structural Design*, San Diego, 575–602.

Ramkumar, R. L., Saether, E. S. and Appa, K. (1986). Strength analysis of laminated and metallic plates bolted together by many fasteners. AFWAL-TR-86-3034.

Ramkumar, R. L., Saether, E. S., Appa, K. and Venkayya, V. B. (1988). Strength analysis of mechanically fastened composite structures. *Behavior and Analysis of Mechanically Fastened Joints in Composite Structures*, AGARD Conference Proc. No. 427, paper No. 7.

Timoshenko, S. P. and Gere, J. M. (1972). *Mechanics of Materials*, Van Nostrand Reinhold Company, New York.

Whitney, J. M. and Nuismer, R. J. (1974). Stress fracture criteria for laminated composites containing stress concentrations. *J. Composite Materials* **8,** 253–265.

Xiong, Y. and Poon, C. (1994). A design model for composite joints with multiple fasteners. Aeronautical Note, IAR-AN-80, NRC No. 32165, National Research Council Canada, Ottawa.